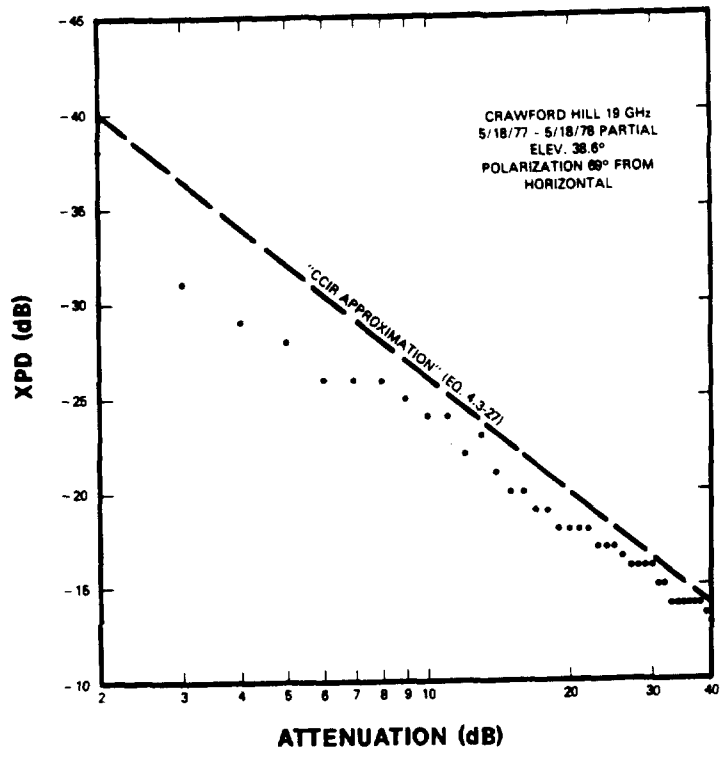

Figure 5.7-1. 19 GHz Cross-Polarization Measurements - Near Vertical Polarization

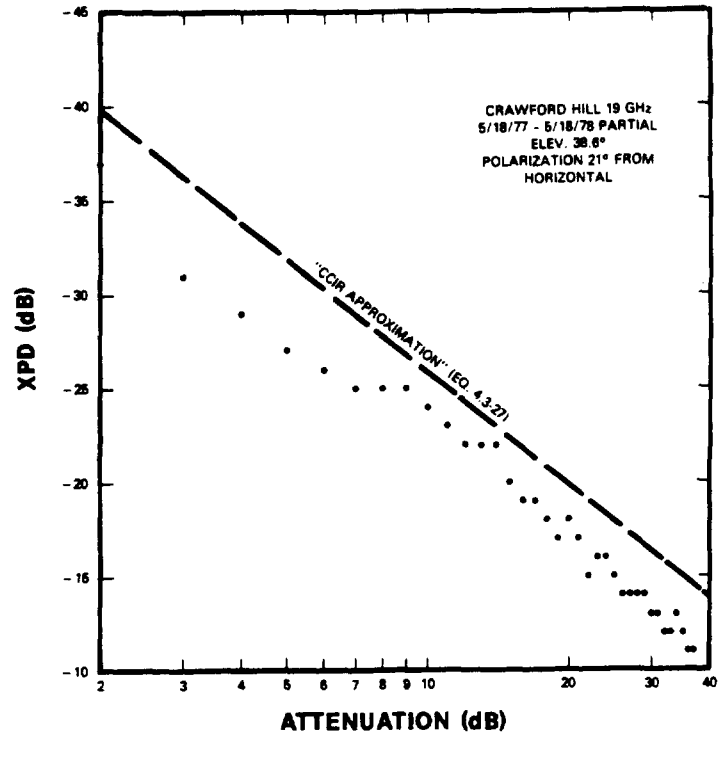

Figure 5.7-2. 19 GHz Cross-Polarization Measurements - Near Horizontal Polarization

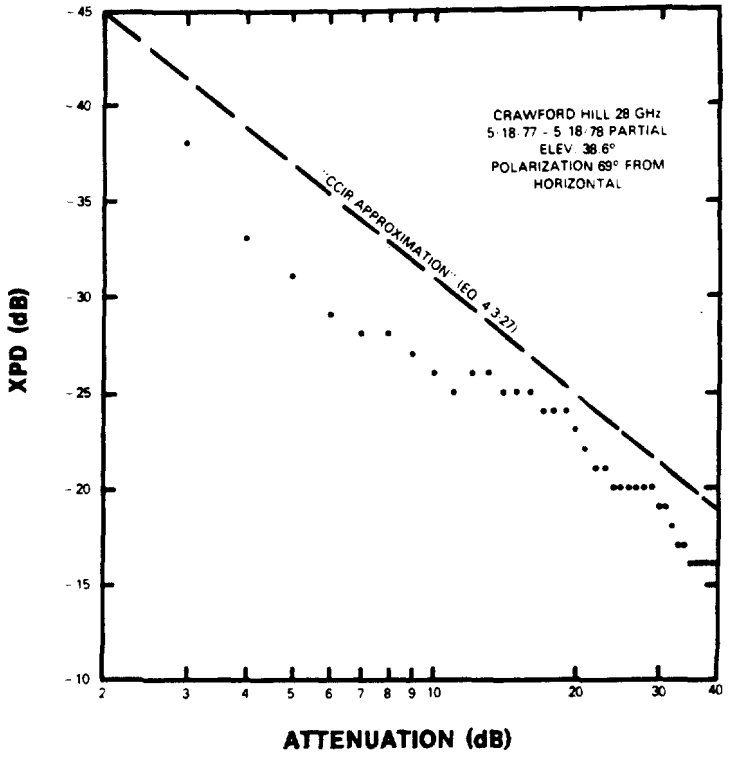

Figure 5.7-3. 28 GHZ Crosspolarization Measurements

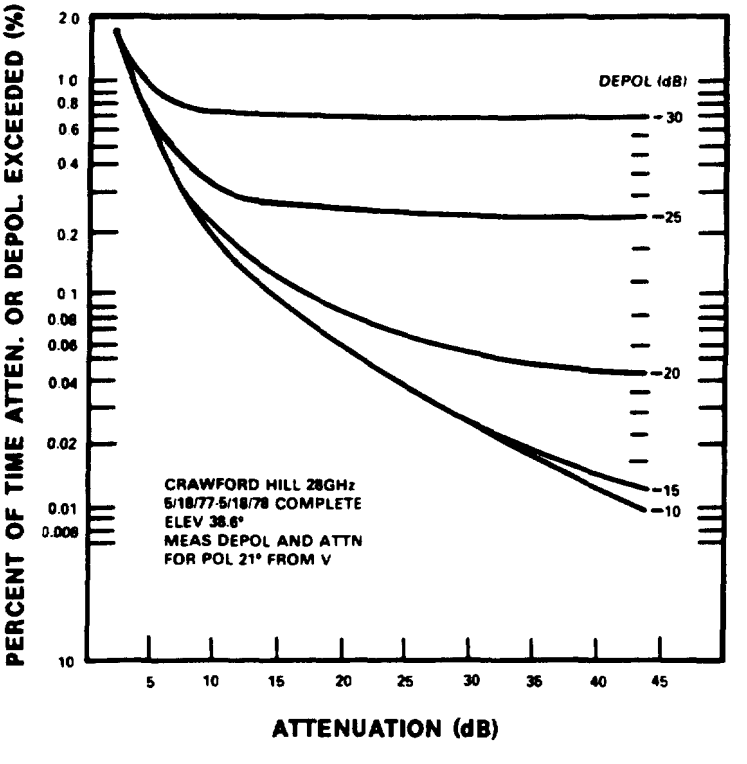

Figure 5.7-4. Joint Attenuation-Depolarization Statistics for 28 GHz Link

A family of curves of the type shown in Figure 5.7-4 gives the outage percentage for a hypothetical system that is unavailable when either an attenuation or an XPD threshold is passed. This is a useful approximation, although most systems allow for some tradeoff between XPD and attenuation. When attenuation is low, for example, greater crosstalk may be tolerable than when attenuation is appreciable.

5.8 PHASE AND AMPLITUDE DISPERSION

Experimental measurements of the phase and amplitude dispersion in the lower troposphere made from the COMSTAR D2 satellite have been made at Crawford Hill, NJ (Cox, et al-1979b). The measurements were made across the 528 MHz coherent sidebands at 28 GHz and between the 19 and 28 GHz carriers which were coherent.

The nine-month Crawford Hill data set has been comprehensively searched for evidence of phase dispersion. For all propagation events, the change in average sideband to carrier phase is less than the measurement uncertainty of about 13° for attenuation up to 45 dB. Phase fluctuations are consistent with signal-to-noise ratios over the 45 dB attenuation range. The change in average 19 to 28 GHz phase is on the order of 60° over a 30 dB attenuation range at 28 GHz. This average phase change appears to be due only to the average dispersive properties of the water in the rain along the path. There is no evidence of multipath type dispersion.

Attenuation in dB at 28 GHz is 2.1 times greater than that at 19 GHz for attenuations up to 29 dB at 19 GHz. The small spread observed in the relationship between 19 and 28 GHz attenuations is consistent with the absence of significant phase dispersion over the 528 MHz bandwidth.

5.9 REFERENCES

Arnold, H.W., D.C. Cox, H.W. Hoffman and R.P. Leck (1979), "Characteristics of Rain and Ice Depolarization for a 19 and 28 GHz Propagation Path from a COMSTAR Satellite," Conference Record, ICC 79, Vol. 3, Boston, MA pp 40.5.1-6.

Arnold, H.W., D.C. Cox, and A.J. Rustako, Jr. (1980), "Rain Attenuation at 10-30 GHz Along Earth-Space Paths: Elevation Angle, Frequency, Seasonal and Diurnal Effects, "Conference Record, ICC 80, Seattle, WA, Vol. 3, pp. 40.3.1-7.

Bostian, C.W., et al (1979), "A Depolarization and Attenuation Experiment Using the COMSTAR and CTS Satellites," Virg. Poly. Inst. and State Univ., Annual Report, NASA Cont. NAS5-22577.

Brussaard, G. (1977), "Rain Attenuation on Satellite-Earth Paths at 11.4 and 14 GHz, "URSI Commission F Symposium Proceedings, April 28 - May 6, 1977 La Baule, France.

CCIR (1978) "Rain Attenuation Prediction " Document P/105-E, CCIR Study Groups Special Preparatory Meeting (WARC-79), International Telecommunications Union, Geneva.

CCIR (1986a), "Propagation Data and Prediction Methods Required for Space Telecommunications Systems," Report 564-3, in Volume V, Recommendations and Reports of the CCIR - 1986, International Telecommunications Union, Geneva, ISBN No. 92-61-02741-5, NTIS Accession No. PB-87-14116-4.

CCIR (1986b), "Data Banks Used for Testing Prediction Methods in Sections E, F and G of Volume V," Document 5/378 (Rev.1), International Telecommunications Union, Geneva.

Chu, T.S. (1974), "Rain Induced Cross-Polarization at Centimeter and Millimeter Wavelengths," BSTJ, Vol. 53, pp 1557-79.

Cox, D.C., H.W. Arnold and A.J. Rustako, Jr. (1979a), "Attenuation and Depolarization by Rain and Ice Along Inclined Radio Paths Through the Atmosphere at Frequencies Above 10 GHz," Conference Record, EASCON 79, Arlington, VA, Vol. 1, pp 56-61.

Cox, D.C., H.W. Arnold and R.P. Lick (1979b), "Phase and Amplitude Dispersion for Earth-Space Propagation in the 20 to 30 GHz Frequency Range," URSI Program and Abstracts, Spring Meeting, Seattle, Washington, June 18-22, p 253.

Crane, R.K. (1980), "Prediction of Attenuation by Rain," IEEE Trans. on Comm., Vol. COM-28, No. 9, pp. 1717-1733.

Davies, P.G. (1976), "Diversity Measurements of Attenuation at 37 GHz with Sun-Tracking Radiometers in a 3-site Network," Proc IEEE, Vol. 123, page 765.

Davies, P.G., M.J. Courthold and E.C. MacKenzie (1981), "Measurements of Circularly-Polarized Transmissions from the OTS and SIRIO Satellites in the 11 GHz Band," IEE Conference Publication No. 195, Internat. Conf. Ant. Prop., York, U.K., April 1981.

Fukuchi, H., M. Fujita, K. Nakamura, Y. Furuhama, and Y. Otsu (1981), "Rain Attenuation Characteristics on Quasi-Millimeter Waves Using Japanese Geostationary Satellites CS and BSE," IEEE Conference Publication No. 195, Internat. Conf. Ant. Prop., York, U.K., April 1981.

Goldhirsh, J. (1979), "Cumulative Slant Path Rain Attenuation Statistics Associated with the Comstar Beacon at 28.56 GHz for Wallops Island, VA," IEEE, Trans. Ant. Prop., Vol. AP-27, No. 6, pp 752-758.

Goldhirsh, J. (1980), "Multiyear Slant-Path Rain Fade Statistics at 28.56 GHz for Wallops Island, VA," IEEE Trans. Ant. Prop., Vol. AP-28, No. 6, pp. 934-941.

Goldhirsh, J. (1982), "Space Diversity Performance Prediction for Earth-Satellite Paths using Radar Modeling Techniques," Radio Science, Vol. 17, No. 6, pp. 1400-1410.

Hayashi, R., Y. Otsu, Y. Furuhama, and N. Fugono (1979), "Propagation Characteristics on Millimeter and Quasi-Millimeter Waves by Using Three Geostationary Satellites of Japan," paper IAF-79-F-281, XXX Congress, International Astronautical Federation, Munich, Germany.

Ippolito, L.J. (1978), "11.7 GHz Attenuation and Rain Rate Measurements With the Communications Technology Satellite (CTS)," NASA Tech. Memo. 80283, Greenbelt, MD.

Kaul, R., D. Rogers and J. Bremer (1977), "A Compendium of Millimeter Wave Propagation Studies Performed by NASA," ORI Tech. Rpt., NASA Contract NAS5-24252.

Kumar, P.N. (1982), "Precipitation Fade Statistics for 19/29 - GHz Comstar Beacon Signals and 12-GHz Radiometric Measurements," COMSAT Technical Review, Vol. 12, No. 1, pp. 1-27.

Lin, S.H., H.J. Bergmann, and M. V. Pursley (1980) "Rain Attenuation on Earth-Satellite Paths - Summary of 10-Year Experiments and Studies," BSTJ, Vol. 59, No. 2, pp. 183-228.

Macchiarella, G. and M. Mauri (1981), "Statistical Results on Centimetric Waves Propagation after Two Years of Activity with the Italian Satellite SIRIO," URSI Commission F Open Symposium, Lenoxville, Canada, May 1980.

Nackoney, O.G. (1979), "CTS 11.7 GHz Propagation Measurements, Third Year's Data and Final Report," GTE Laboratories Report TR-79-471.2, Waltham, MA.

Nowland, W.L., R.L. Olsen and I.P. Shkarofsky, (1977), "Theoretical Relationship Between Rain Depolarization and Attenuation," Electronics Letters, Vol. 13, No. 22, pp 676-7.

Ramat, P. (1980), "Propagation Oblique dans les Bandes de Frequences des 11 et 14 GHz," URSI Commission F Open Symposium, Lenoxville, Canada, May 1980.

Rice, P.L. and N.R. Holmberg (1973), "Cumulative Time Statistics of Surface Point Rainfall Rates," IEEE Trans. Comm., Vol. COM-21 pp 1131-1136.

Rogers, D. V. (1981), "Diversity- and Single-Site Radiometric Measurements of 12-GHz Rain Attenuation in Different Climates," IEEE Conference Publication No. 195, Internat. Conf. Ant. Prop., York, U.K., April 1981.

Rogers, D. V. and G. Hyde (1979), "Diversity Measurements of 11.6 GHz Rain Attenuation at Etam and Lenox, West Virginia," COMSAT Tech. Rev., Vol. 9, No. 1, pp. 243-254.

Rucker, F. (1980), "Simultaneous Propagation Measurements in the 12-GHz Band on the SIRIO and OTS Satellite Links," URSI Commission F Open Symposium, Lenoxville, Canada, May 1980.

Rustako, A.J., Jr. (1979), "Measurement of Rain Attenuation and Depolarization of the CTS Satellite Beacon at Holmdel, New Jersey," 1979 USNC/URSI Meeting, June 18-22, Seattle WA (abstract).

Vogel, W.J. (1979), "CTS Attenuation and Cross Polarization Measurements at 11.7 GHz," Univ. Texas Austin, Final Fpt., NASA Contract NAS5-22576.

Vogel, W.J. (1982), "Measurement of Satellite Beacon Attenuation at 11.7, 1904, and 28.56 GHz and Radiometric Site Diversity at 13.6 GHz," Radio Science, Vol. 17, No. 6, pp. 1511-1520.

CHAPTER VI

PREDICTION TECHNIQUES

6.1 INTRODUCTION

6.1.1 Purpose

This chapter provides a guide to prediction methods and related propagation results for the evaluation of earth-space paths operating above 10 GHz. The topics covered are:

Gaseous Attenuation

Rain Attenuation

Cloud, Fog, Sand and Dust Attenuation

Signal Fluctuations and Low Angle Fading

Depolarization Effects

Bandwidth Coherence

Sky Noise

The techniques described here have been developed from recent ongoing NASA supported studies and from the relevant published literature. These techniques represent the state of knowledge of the adverse effects of the earth's atmosphere on reliable earth-space transmissions above 10 GHz.

This chapter provides propagation data in a format suitable for use by earth-space link system designers operating in the frequency range from 10 to 100 GHz. In this frequency range the troposphere can have a significant effect on the carrier-to-noise ratio of a propagating wave. Typically, the troposphere attenuates and depolarizes the carrier signal and adds broadband amplitude and

phase noise to the signal. The resulting carrier-to-noise ratio reduction reduces the allowable data rate for a given bit error rate (digital systems) and the quality of transmission (analog systems). In the most severe cases the medium will significantly attenuate the carrier and destroy the transmission capabilities of the link (termed a link outage). The frequency of occurrence and average outage time per year are usually of most interest to system designers. Propagation studies to date now allow the predictions to be made with a high degree of certainty and have developed means to reduce the frequency and length of these outages.

6.1.2 Organization of This Chapter

The remainder of this chapter is arranged in six relatively independent sections covering the key topics related to the interaction of the troposphere and earth-space propagation paths. Each section presents a description of selected techniques and provides sample calculations of the techniques applied to typical communications systems parameters. A guide to the sample calculations is given in Table 6.1-1.

6.1.3 Frequency Bands for Earth-Space Communication

Within the guidelines established by the International Telecommunication Union (ITU) for Region 2 (includes U.S. and Canada), the Federal Communications Commission (FCC) in the U.S. and the Department of Communications (DOC) in Canada regulate the earth-space frequency allocations. In most cases, the FCC and DOC regulations are more restrictive than the ITU regulations.

The services which operate via earth-space links are listed in Table 6.1-2. The definitions of each of these services are given in the ITU Radio Regulations. The specific frequency allocations for these services are relatively fixed, but modifications can be enacted at World Administrative Radio Conferences based on the proposals of ITU member countries.

Table 6.1-1. Guide to Sample Calculations

A review of the Radio Regulations indicates that most of the frequency spectrum above 10 GHz is assigned to the satellite services or the radio astronomy service. This does not mean that the FCC or DOC will utilize them as such, but it does highlight the potential for use of these frequency bands. Figure 6.1-1 shows those frequency segments not assigned for potential use by the services listed in Table 6.1-2 (ITU-1980).

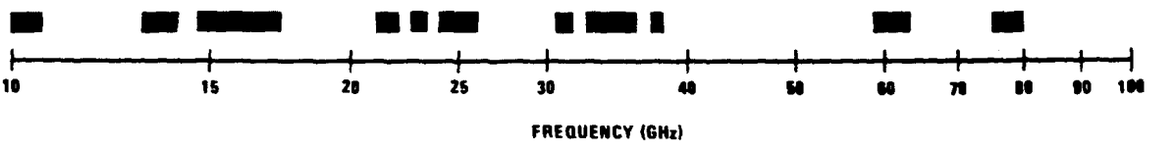

Figure 6.1-1. Frequencies Not Allocated Primarily for Earth-Space Transmissions in Region 2

Table 6.1-2. Telecommunication Services Utilizing Earth-Space Propagation Links

Fixed Satellite
Mobile Satellite
Aeronautical Mobile Satellite
Maritime Mobile Satellite
Land Mobile Satellite
Broadcasting Satellite
Radionavigation Satellite
Earth Exploration Satellite
Meteorological Satellite
Amateur Satellite
Standard Frequency Satellite
Space Research
Space Operations
Radio Astronomy

6.1.4 Other Propagation Effects Not Addressed in This Chapter

6.1.4.1 Ionospheric Effects. The ionosphere generally has a small effect on the propagation of radio waves in the 10 to 100 GHz range, Whatever effects do exist (scintillation, absorption, variation in the angle of arrival, delay, and depolarization) arise due to the interaction of the radio wave with the free electrons, electron density irregularities and the earth's magnetic field. The density of electrons in the ionosphere varies as a function of geomagnetic latitude, diurnal cycle, yearly cycle, and solar cycle (among others). Fortunately, most U.S. ground station-satellite paths pass through the midlatitude electron density region, which is the most homogeneous region. This yields only a small effect on propagation. Canadian stations may be affected by the auroral region electron densities which are normally more irregular. A more complete discussion of the effects is included in Report 263-6 of CCIR Volume VI (1986a).

A mean vertical one-way attenuation for the ionosphere at 15 GHz for the daytime is typically 0.0002 dB (Millman-1958), the amplitude scintillations are generally not observable (Crane-1977) and the transit time delay increase over the free space propagation time delay is of the order of 1 nanosecond (Klobuchar-1973). Clearly for most systems operating above 10 GHz these numbers are sufficiently small that other system error budgets will be much larger than the ionospheric contributions.

The one ionospheric effect which might influence wide bandwidth systems operating above 10 GHz is phase dispersion. This topic is discussed in Section 6.7.

6.1.4.2 Tropospheric Delays. Highly accurate satellite range, range-rate and position-location systems will need to remove the propagation group delay effects introduced by the troposphere. Extremely high switching rate TDMA systems require these corrections. The effects arise primarily due to the oxygen and water vapor in the lower troposphere. Typical total additional

propagation delay errors have been measured to be of the order of 8 nanoseconds (Hopfield-1971).

Estimation techniques, based on the measurement of the surface pressure, temperature and relative humidity have been developed (Hopfield-1971, Bean and Dutton-1966, Segal and Barrington-1977) which can readily reduce this error to less than 1 nanosecond. In addition, algorithms for range (Marini-1972a) and range-rate (Marini-1972b) have been prepared to reduce tropospheric contributions to satellite tracking errors.

Since this topic is quite specialized and generally results in an additional one-way delay of less than 10 nanoseconds it is not addressed further in this report. An overview of this subject and additional references are available in CCIR Report 564-3 (1986b), and Flock, Slobin and Smith (1982).

6.2 PREDICTION OF GASEOUS ATTENUATION ON EARTH-SPACE PATHS

The mean attenuation of gases on earth-space paths in the 10 to 100 GHz frequency range has been theoretically modeled and experimentally measured. Above 20 GHz gaseous absorption can have a significant effect on a communication system design depending on the specific frequency of operation. Because of the large frequency dependence of the gaseous absorption, an earth-space communication system designer should avoid the high absorption frequency bands. Alternatively, designers of secure short-haul terrestrial systems can utilize these high attenuation frequency bands to provide system isolation.

6.2.1 Sources of Attenuation

In the frequency range from 10 to 100 GHz the water vapor absorption band centered at 22.235 GHz and the oxygen absorption lines extending from 53.5 to 65.2 GHz are the only significant contributors to gaseous attenuation. The next higher frequency absorption bands occur at 118.8 GHz due to oxygen and 183 GHz due to water vapor. The absorption lines are frequency broadened by

collisions at normal atmospheric pressures (low elevations) and sharpened at high altitudes. Thus the total attenuation due to gaseous absorption is ground station altitude dependent.

6.2.2 Gaseous Attenuation

6.2.2.1 One-Way Attenuation Values Versus Frequency. The Zenith one-way attenuation for a moderately humid atmosphere (7.5 g/m surface water vapor density) at various ground station altitudes (starting heights) above sea level is presented in Figure 6.2-1 and Table 6.2-1. These curves were computed (Crane and Blood, 1979) for temperate latitudes assuming the U.S. Standard Atmosphere, July, 45 N. latitude. The range of values indicated in Figure 6.2-1 refers to the peaks and valleys of the fine absorption lines. The range of values at greater starting heights (not shown) is nearly two orders of magnitude (Leibe-1975).

Table 6.2-1. Typical One-Way Clear Air Total Zenith Attenuation Values, A_c' (dB) (Mean Surface Conditions 21°C, 7.5 g/m^3 H_2O; U.S. Std. Atmos. 45°N., July)

Frequency	ALTITUDE				
	0km*	0.5km	1.0km	2.0km	4.0km
10 GHZ	.053	.047	.042	.033	.02
15	.084	.071	.061	.044	.023
20	.28	.23	.18	.12	.05
30	.24	.19	.16	.10	.045
40	.37	.33	.29	.22	.135
80	1.30	1.08	.90	.62	.30
90	1.25	1.01	.81	.52	.22
100	1.41	1.14	.92	.59	.25

*1 km = 3281 feet

Figure 6.2-1 also shows two values for the standard deviation of the clear air zenith attenuation as a function of frequency. The larger value was calculated from 220 measured atmosphere profiles, spanning all seasons and geographical locations (Crane-1976). The smaller value applies after the mean surface temperature and humidity have been taken into account by making the corrections given below.

6.2.2.1.1 Dependence on Ground Station Altitude. The compensation for ground station elevation can be done to first order by linearly interpolating between the curves in Figure 6.2-1. The zenith one-way attenuation for typical ground station altitudes, found in this way, is tabulated in Table 6.2-1 for easy reference.

6.2.2.1.2 Dependence on Water Vapor Content. The water vapor content is the most variable component of the atmosphere. Therefore, for arid or humid regions, a correction should be made based on the expected mean values of water vapor content when utilizing frequencies between 10 and 50 GHz. This correction to the total zenith attenuation is linearly related to the mean local water vapor density at the surface p :.

$$\Delta A_{c1} = b_\rho \, (\rho_o - 7.5 \text{ g/m}^3) \qquad (6.2\text{-}1)$$

where ΔA_{c1} is an additive correction to the zenith clear air attenuation (given by Figure 6.2-1 and Table 6.2-1) that accounts for the difference between the mean local surface water vapor density and 7.5 g/m^3. The coefficient b_ρ is frequency dependent and is given by Figure 6.2-2 and Table 6.2-2 (Crane ana Blood, 1979). The accuracy of this correction factor is greatest for sea level altitude.

The US and Canadian weather services generally measure relative humidity or the partial pressure of water vapor. The technique for converting these values to ρ_o is given in Section 6.2.5.

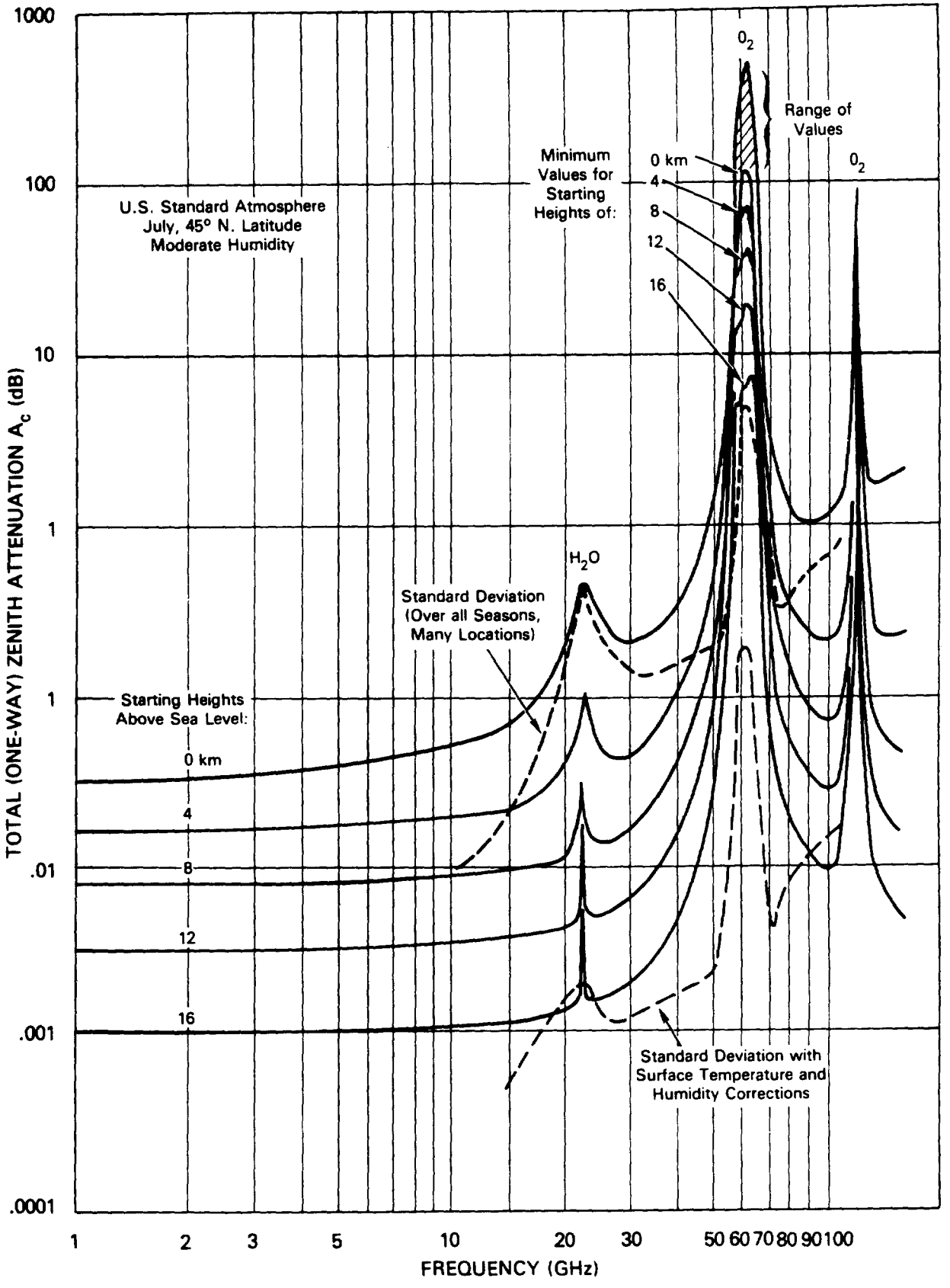

Figure 6.2-1. Total Zenith Attenuation Versus Frequency

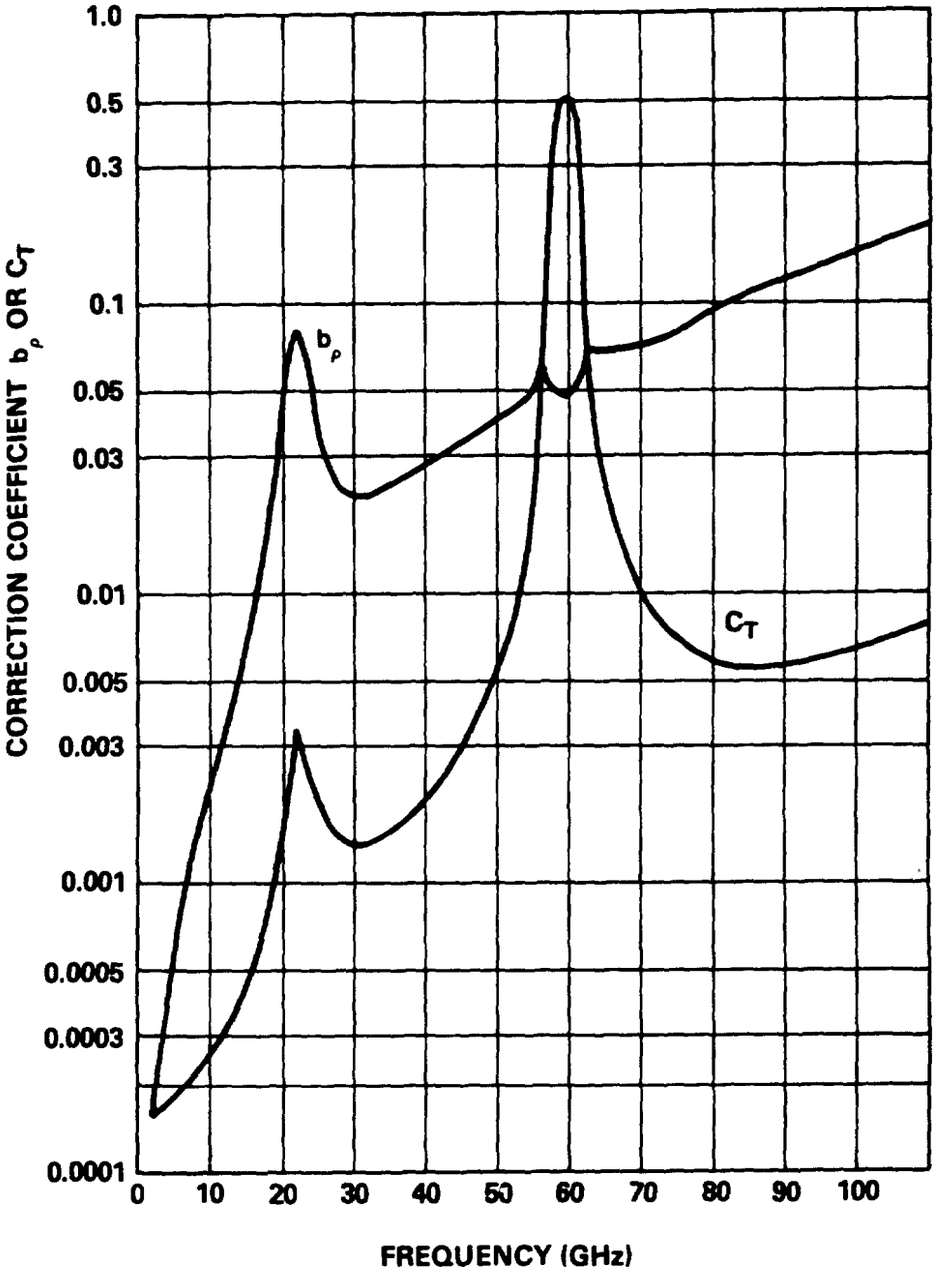

Figure 6.2-2. Water Vapor Density and Temperature Correction Coefficients

Table 6.2-2. Water Vapor Density and Temperature Correction Coefficients

Frequency (GHz)	Water Vapor Density Correction b_ρ	Temperature Correction C_T
10	2.10×10^{-3}	2.60×10^{-4}
15	6.34×10^{-3}	4.55×10^{-4}
20	3.46×10^{-2}	1.55×10^{-3}
30	2.37×10^{-2}	1.33×10^{-3}
40	2.75×10^{-2}	1.97×10^{-3}
80	9.59×10^{-2}	5.86×10^{-3}
90	1.22×10^{-1}	5.74×10^{-3}
100	1.50×10^{-1}	6.30×10^{-3}

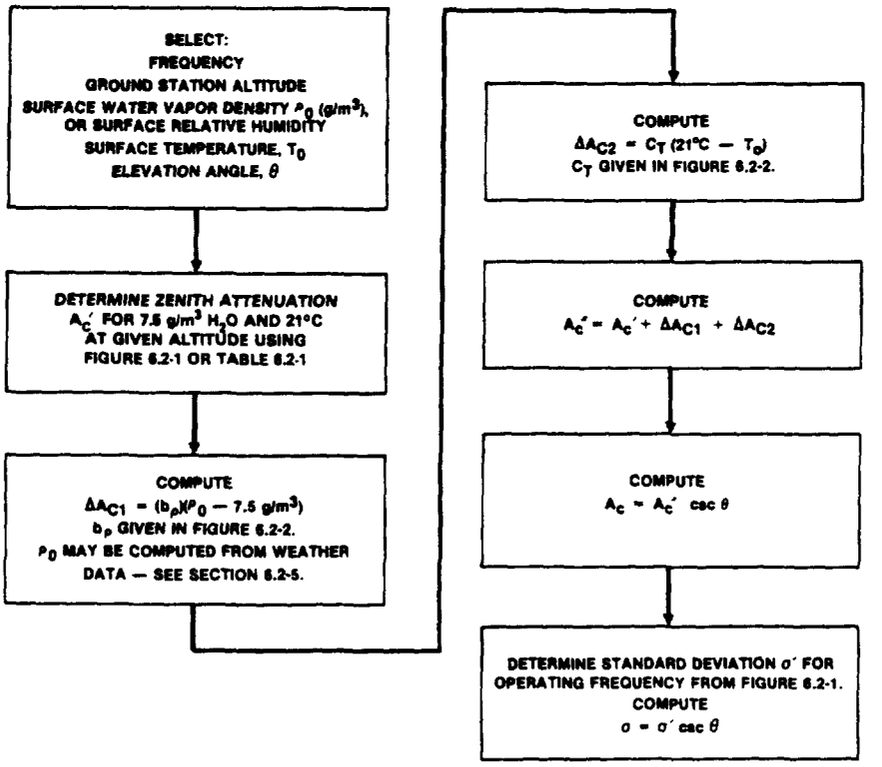

Figure 6.2-3. Technique for Computing Mean Clean Air Attenuation

6.2.2.1.3 Dependence on Surface Temperature. The mean surface temperature T_o also affects the total attenuation. This relation (Crane and Blood, 1979) is also linear:

$$\Delta A_{c2} = c_T \ (21^\circ - T_o) \qquad (6.2\text{-}2)$$

where T_o is mean local surface temperature in °C.

A_{c2} is an additive correction to the zenith clear air attenuation. Frequency dependent values for c_T are given in Figure 6.2-2 and Table 6.2-2. As with water vapor correction, the accuracy of this factor decreases with altitude.

6.2.2.1.4 Dependence on Elevation Angle. For elevation angles greater than 5 or 6 degrees, the zenith clear air attenuation A_c is multiplied by the cosecant of the elevation angle θ. The total attenuation for arbitrary elevation angle is

$$A_c = A_c' \csc \theta \qquad (6.2\text{-}3)$$

The standard deviation (see Figure 6.2-1) also is multiplied by the csc θ for arbitrary elevation angles.

6.2.3 Estimation Procedure For Gaseous Attenuation

The CCIR has developed an approximate method to calculate the median gaseous absorption loss expected for a given value of surface water vapor density, (CCIR-1986a). The method is applicable up to 350 GHz, except for the high oxygen absorption bands.

Input parameters required for the calculation are:

f - frequency, in GHz

θ - path elevation angle, in degrees,

h_s - height above mean sea level of the earth terminal, in km, and

ρ_w - water vapor density at the surface, for the location of interest, in g/m^3.

If ρ_w is not available from local weather services, representative median values can be obtained from CCIR Report 563-3 (CCIR-1986c).

The specific attenuation at the surface for dry air (P = 1013 mb) is then determined from:

$$\gamma_o = \left[7.19 \times 10^{-3} + \frac{6.09}{f^2 + 0.227} + \frac{4.81}{(f - 57)^2 + 1.50} \right] f^2 \times 10^{-4} \text{ dB/km}$$

$$\text{for } f < 57 \text{ GHz} \qquad (6.2\text{-}4)$$

$$\gamma_o = \left[3.79 \times 10^{-7} f + \frac{0.265}{(f - 63)^2 + 1.59} + \frac{0.028}{(f - 118)^2 + 1.47} \right] \times (f^2 + 198)^2 \times 10^{-3} \text{ dB/km}$$

$$\text{for } 63 < f < 350 \text{ GHz}$$

[The application of the above relationships in the high oxygen absorption bands (50-57 GHz and 63-70 GHz) may introduce errors of up to 15%. More exact relationships are given in CCIR Report 719 (CCIR-1986d)].

The specific attenuation for water vapor, γ_w, is found from:

$$\gamma_w = \left[0.067 + \frac{3}{(f - 22.3)^2 + 7.3} + \frac{9}{(f - 183.3)^2 + 6} + \frac{4.3}{(f - 323.8)^2 + 10} \right] f^2 \rho_w \, 10^{-4} \text{ dB/km} \qquad (6.2\text{-}5)$$

$$\text{for } f < 350 \text{ GHz}$$

The above expressions are for an assumed surface air temperature of 15°C. corrections for other temperatures will be described later. Also, the above results are accurate for water vapor densities less than 12 g/m^3. [For higher water vapor density values, see CCIR Report 719 (CCIR-1986d), and the following.]

An algorithm for the specific attenuation of water vapor which includes a quadratic dependence on water vapor density and allows

values of water vapor densities >12 g/m³, has been proposed by Gibbons (1986) and provisionally accepted by the CCIR (1988),

$$\gamma_w = \left[0.050 + 0.0021\rho_w + \frac{3.6}{(f - 22.2)^2 + 8.5} + \frac{10.6}{(f - 183.3)^2 + 9.0} + \frac{8.9}{(f - 325.4)^2 + 26.3} \right] f^2 \rho_w 10^{-4} \quad \text{dB/km} \tag{6.2-6}$$

for $T = 15^{\circ}C$ and $f < 350$ GHz.

Gibbons finds Eq. (6.2-6) to be valid within about ± 15% over the range of ρ_w from 0 to 50 g/m³. However, in applying Eq. (6.2-6) with water vapor densities greater than 12 g/m³ it is important to remember that the water vapor density may not exceed the saturation value ρ_s at the temperature considered. This saturation value may be expressed as (Gibbons, 1986),

$$\rho_s = 17.4\left(\frac{300}{T}\right)^6 10^{\left(10 - \frac{2950.2}{T}\right)} \quad \text{g/m}^3 \tag{6.2-7}$$

where T is the temperature in °K.

For temperatures in the range -20°C to +40°C Gibbons proposes a temperature dependence of -1.0% per °C for dry air in the window regions between absorption lines and -0.6% per °C for water vapor. The correction factors are therefore

$$\gamma_o = \gamma_o(15\ ^{\circ}C)\left[1 - 0.01(T_o - 15)\right] \tag{6.2-8}$$

$$\gamma_w = \gamma_w(15\ ^{\circ}C)\left[1 - 0.006(T_o - 15)\right] \tag{6.2-9}$$

where T_o is the surface temperature in °C.

The equivalent heights for oxygen, h_o, and water vapor, h_w, are determined from:

$$h_o = 6 \quad \text{km} \qquad \text{for } f < 57 \text{ GHz} \tag{6.2-10}$$

$$h_o = 6 + \frac{40}{(f - 118.7)^2 + 1} \quad \text{km} \qquad \text{for } 63 < f < 350 \text{ GHz}$$

$$h_w = \left[2.2 + \frac{3}{(f - 22.3)^2 + 3} + \frac{1}{(f - 183.3)^2 + 1} + \frac{1}{(f - 323.8)^2 + 1} \right] \quad \text{km} \qquad \text{for } f < 350 \text{ GHz} \tag{6.2-11}$$

The total slant path gaseous attenuation through the atmosphere, A_g, is then found.

For $\theta \geq 10°$:

$$A_g = \frac{\gamma_o h_o e^{-\frac{h_s}{h_o}} + \gamma_w h_w}{\sin \theta} \quad \text{dB} \tag{6.2-12}$$

For $\theta < 10°$:

$$A_g = \frac{\gamma_o h_o}{g(h_o)} + \frac{\gamma_w h_w}{g(h_w)} \quad \text{dB} \tag{6.2-13}$$

with

$$g(h) = 0.661x + 0.339\sqrt{x^2 + \frac{h}{1545.5}} \tag{6.2-14}$$

$$x = \sqrt{\sin^2 \theta + \frac{h_s}{4250}} \tag{6.2-15}$$

where h is replaced by h_o or h_w as appropriate.

The above procedure does not account for contributions from trace gases. These contributions are negligible except in cases of very low water vapor densities ($\leq$1 g/m^3) at frequencies above about 70 GHz.

6.2.4 Conversion of Relative Humidity to Water Vapor Density

The surface water vapor density ρ_o (g/m^3) at a given surface temperature T_o may be found from the ideal gas law

$$\rho_o = (R.H.)\ e_s/R_w(T_o + 373) \qquad (6.2\text{-}16)$$

where R.H. is the relative humidity, e_s (N/m^2) is the saturated partial pressure of water vapor corresponding to the surface temperature T_o($^\circ$C) and R_w = 461 joule/kgK = 0.461 joule/gK. A plot of e_s in various units is given in Figure 6.2-4. For example, with

R.H. = 50% = 0.5

T_o = 20°C

$e_s \simeq$ 2400 n/m^2 at 20°C from Figure 6.2-4

then

ρ_o = 8.9 g/m^3.

The relative humidity corresponding to 7.5 g/m^3 at 20°C (68°F) is R.H. = 0.42 = 42%.

6.2.5 A Sample Calculation for Gaseous Attenuation

This section presents an example calculation for the total path gaseous attenuation, using the CCIR procedure described in Section 6.2.3.

Assume the following input parameters for a K_a band link:

Frequency, f = 29.3 GHz

Path Elevation Angle, θ = 38°

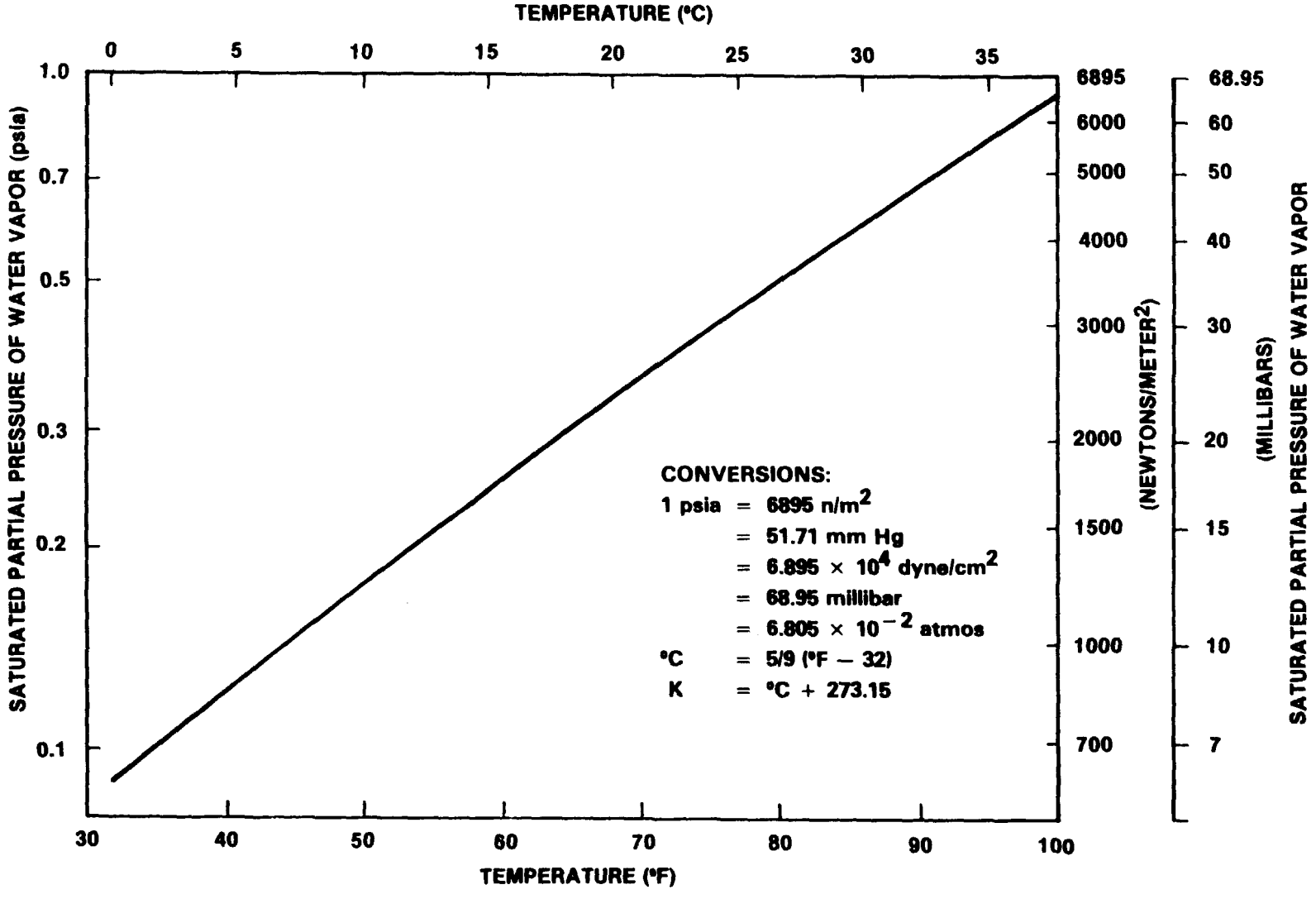

Figure 6.2-4. The Saturated Partial Pressure of Water Vapor Versus Temperature

Height above mean sea level, h_s = .2 km

Surface water vapor density, ρ_w = 7.5 g/m^3

Surface temperature, T_o = 20°C

Step 1. Calculate the specific attenuation coefficients for oxygen, γ_o, and for water vapor, γ_w, from Equations (6.2-4) and (6.2-6) respectively;

γ_o = 0.01763 dB/km (from f<57 GHz relationship)
γ_w = 0.0777 dB/km

Step 2. Correct γ_o and γ_w for 20°C, using equations (6.2-8) and (6.2-9) respectively;

γ_o = 0.01763 [1-0.01(20-15)] = 0.01675 dB/Km
γ_w = 0.0777 [1-0.006(20-15)] = 0.07537 dB/Km

Step 3. Calculate the equivalent heights for oxygen, h_o, and for water vapor, h_w, from Equations (6.2-10) and (6.2-11) respectively;

h_o = 6 km
h_w = 2.258 km

Step 4. The total slant path gaseous attenuation is determined from Equation (6.2-8);

$$A = [(0.018)\ (6)e^{-(0.2)/(6)} + (0.078)\ (2.258)]/\sin(38)$$
$$= 0.1579 + 0.2764 = 0.4343 \text{ dB}$$

The results show that the contribution from oxygen absorption is 0.1579 dB, and the contribution from water vapor is 0.2764 dB, for a total of 0.4343 dB.

6.3 PREDICTION OF CUMULATIVE STATISTICS FOR RAIN ATTENUATION

6.3.1 General Approaches

6.3.1.1 Introduction to Cumulative Statistics. Cumulative statistics give an estimate of the total time, over a long period, that rain attenuation or rate can be expected to exceed a given amount. They are normally presented with parameter values (rain rate or attenuation) along the abscissa and the total percentage of time that the parameter value was exceeded (the "exceedance time") along the ordinate. The ordinate normally has a logarithmic scale to most clearly show the exceedance times for large values of the parameter, which are often most important. Usually, the percentage exceedance time is interpreted as a probability and the statistical exceedance curve is taken to be a cumulative probability distribution function. Because of the general periodicity of meteorological phenomena, cumulative statistics covering several full years, or like periods of several successive years, are the most directly useful. (A technique exists, however, for extending statistics to apply to periods greater than those actually covered. This is described in Section 6.3.4.) Statistics covering single years or periods would be expected to exhibit large fluctuations from year to year, because of the great variability of the weather. In most geographic regions, data covering ten years or more is usually required to develop stable and reliable statistics.

Cumulative rain rate or attenuation exceedance statistics alone give no information about the frequency and duration of the periods of exceedance. Rather, only the total time is given. The nature of rain attenuation, however, is such that the exceedance periods are usually on the order of minutes in length. Different phenomena besides rain give rise to attenuation variations occurring on a time scale of seconds. These amplitude scintillations, as they are called, are not considered in this section, but are discussed in Section 6.5.